

A Complete LTspice Simulation Model for SAW Devices

Alper ŞİŞMAN ¹ 

¹Marmara Üniversitesi, Mühendislik Fakültesi, Elektrik ve Elektronik Mühendisliği Bölümü, 34722, İstanbul, Türkiye

Abstract

A complete circuit model of Surface Acoustic Wave (SAW) devices with straight interdigital transducers is presented. This equivalent circuit can be implemented in LTspice and contains variable design characteristics that can be easily changed to see their effect on the electrical response of the final SAW device design. Later a two port Surface Acoustic Wave device with 13-finger-IDT electrodes is fabricated and its electrical characterization is examined using a vector network analyzer. The test results are then compared with the equivalent circuits' simulation output results for the verification. The results show an acceptable agreement between the experimental and simulation results for a wide frequency range. This paper offers an easy method to create an equivalent LTSpice model to determine the electrical response of a SAW device before fabrication. The model can also be used to simulate the behaviour of the circuits containing SAW devices using LTSPICE tool.

Keywords: SAW Device, LT Spice model, SAW Filter, Equivalent Model.

I. INTRODUCTION

Surface acoustic wave devices have found their applications in many fields of science and technology [1-4]. Since it is imperative to optimize the design parameters before fabrication, having a model to simulate the design accurately offers numerous advantages. Modeling the device opens the path to examining electrical behavior and clarifies whether the design satisfies the expectations. The models in the literature works fine around the resonance frequency and it is difficult to use them with circuit simulation softwares like LTSpice [5, 6]. As a result, it is of a great importance to have a model that is completely electrical and has the capacity to be implemented in electrical simulation programs [7]. Another important point to note is that the equivalent circuit must be able to explain the performance of the device in a wide frequency range [8]. Three important approaches were reported to model the piezo electric based devices: 1-Mason equivalent circuit model, 2-Butterworth Van-Dyke equivalent circuit model. 3- frequency response approach. Other methods employ finite element modeling techniques, which prove beneficial for simulating both sensors and actuators [9,10].

1.1. Mason equivalent circuit model

Most of the equivalent circuit methods for modeling the SAW devices are based on the equivalent circuit theory of Mason [11] where each finger of an IDT device is modeled as a 3-port network [12] shown in Figure 1.

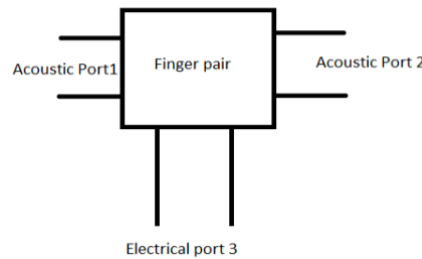


Figure 1. Three port network representation of a finger pair in an IDT

Each finger pair is considered as a 3-port unit that receives and propagates acoustic wave from acoustic ports and is connected to the source through the electrical port. For each IDT pair, these 3-port networks are connected to each other, and the connection is in series configuration acoustically and in parallel configuration electrically. A resistance terminates the last two fingers of the IDT from both left and right sides. This resistance (Z_0) represents the piezoelectric material resistivity to the acoustic wave and the fact that the produced acoustic wave propagates out of or into the IDT from left and right.

The value of that resistor [13] can be determined by (1).

$$Z_0 = \frac{1}{f_0 C_s k^2} \tag{1}$$

Here, f_0 , C_s and k shows operation frequency, capacitance per length of the piezoelectric material and wave number respectively. When a number of finger pairs are connected to each other, the resulting network is shown in figure 2.

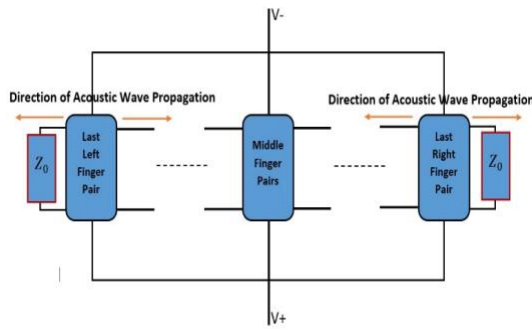


Figure 2. The 3-port networks connected to each other. Acoustic ports are connected in cascade and electrically each block is parallel to the other.

The equivalent circuit of each unit (finger pair) is given by Mason solving for the boundary conditions of each port. Basically, it must be possible to find the admittance matrix of each port however the two-dimensional nature of the problem complicates the calculations, and two approximations are suggested. In the first approximation the electric field is applied in the direction of acoustic wave propagation called the “in line” model and in the next approximation, the electric field is applied perpendicular to the acoustic ports and the direction of acoustic wave propagation called the “crossed field” model. Real electric field and the approximations [14] are shown in figure 3.

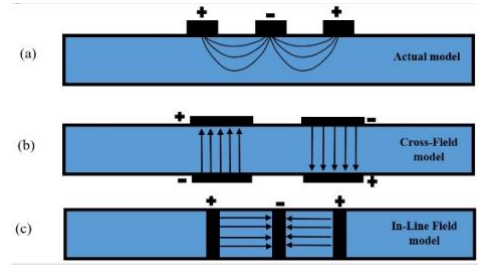


Figure 3. a) Field patterns in a saw device, side view. b) Crossed field approximation. c) In-line approximation

Considering the cross-filed approximation, one can solve [15] the resulting two port linear network of a finger in figure 4, where V^+ and V^- represents transmitted and reflected voltages for input and output sides. I_1 and I_2 are the input and output currents.

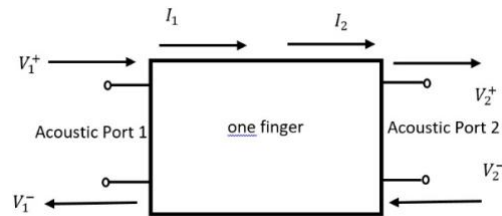


Figure 4. Two port representation of a finger with its voltages and currents.

The expressions (2)-(4) are written according to the network theorem for the two-port networks (figure 4). Here, Z_0 shows the corresponding impedance (note that, port-1 and port-2 are identical). V^+ and V^- represents transmitted and reflected voltages. ‘I’ shows the current and the indices ‘1’ and ‘2’ represents input and output parameters respectively in all equations. S_{11} , S_{12} , S_{21} and S_{22} show the ‘s parameters’ for the two-port network.

$$V_1 = V_1^+ + V_1^- \tag{2a}$$

$$V_2 = V_2^+ + V_2^- \tag{2b}$$

$$I_1 = \frac{1}{z_0} (V_1^+ - V_1^-) \tag{3a}$$

$$I_2 = \frac{1}{z_0} (V_2^+ - V_2^-) \tag{3b}$$

Using network theorem:

$$\begin{bmatrix} V_1^- \\ V_2^+ \end{bmatrix} = \begin{bmatrix} S_{11} & S_{12} \\ S_{21} & S_{22} \end{bmatrix} \begin{bmatrix} V_1^+ \\ V_2^- \end{bmatrix} \tag{4}$$

If the ports of the network are assumed to be perfectly matched, then $S_{11} = S_{22} = 0$.

Assuming no attenuation between the ports and only taking the phase change between ports into consideration $S_{12} = S_{21} = e^{-jkl}$, where k , l and j represents wave number, the distance between two adjacent fingers and the square root of minus one respectively.

as a result, $S = \begin{bmatrix} 0 & e^{-jkl} \\ e^{-jkl} & 0 \end{bmatrix}$ and

$$V_1^- = e^{-jkl} V_2^- \quad (5)$$

$$V_2^+ = e^{-jkl} V_1^+ \quad (6)$$

Since we know that $V_2 = V_2^+ + V_2^-$ (2b) then:

$$V_2 = e^{-jkl} V_1^+ + e^{jkl} V_1^- \quad (7)$$

Use expressions (2a) and (3a),

$$V_2 = V_1 \cos kl - jZ_0 I_1 \sin kl \quad (8)$$

From equation (3b), $I_2 Z_0 = V_2^+ - V_2^-$,

$$I_2 Z_0 = V_2^+ - V_2^- = e^{-jkl} V_1^+ - e^{jkl} V_1^-$$

Use equations (2a) and (3a),

$$I_2 Z_0 = I_1 Z_0 \cos kl - jV_1 \sin kl \quad (9)$$

The matrix is then formed as:

$$\begin{bmatrix} V_2 \\ I_2 \end{bmatrix} = \begin{bmatrix} \cos kl & -jZ_0 \sin kl \\ \frac{-j \sin kl}{Z_0} & \cos kl \end{bmatrix} \begin{bmatrix} V_1 \\ I_1 \end{bmatrix}$$

By arranging the matrix to connect voltage and current variables, ($[Z]$ matrix),

$$\begin{bmatrix} V_1 \\ V_2 \end{bmatrix} = Z_0 \begin{bmatrix} -j \cot kl & j \csc kl \\ -j \csc kl & j \cot kl \end{bmatrix} \begin{bmatrix} I_1 \\ I_2 \end{bmatrix}$$

$$\text{Where } [Z] = \begin{bmatrix} Z_{11} & Z_{12} \\ Z_{21} & Z_{22} \end{bmatrix}$$

Having this Z matrix, we can design a 2-port network with 3 impedances to represent the system. Later when the values of the impedances are calculated and the 2-port network approximation is done, the third port can be added to the system.

The simplest two-port network has three impedances in the form of a T network shown in figure 5. Using network theory and the Z matrix, the value of the network elements are calculated as follows:

when V_2 is open circuited ($I_2 = 0$) according to the Z matrix:

$$V_1 = Z_{11} I_1 \quad (10)$$

$$V_2 = Z_{21} I_1 \quad (11)$$

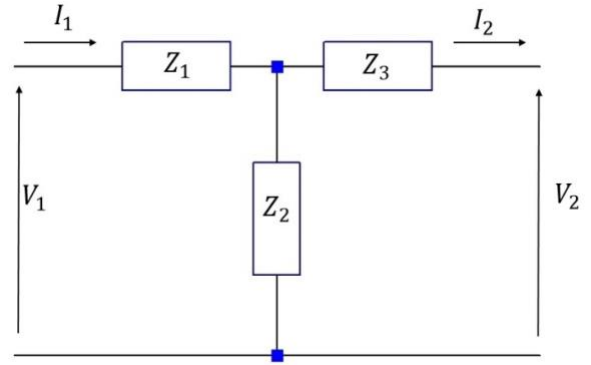


Figure 5. The simplest 2port network with T configuration representing 1-finger model. Here Z_1 , Z_2 and Z_3 represents the impedances in the 1-finger model.

According to figure 5:

$$V_1 = (Z_1 + Z_2) I_1 \quad (12)$$

$$Z_{11} = Z_1 + Z_2 \quad (13)$$

$$-j Z_0 \cot kl = Z_1 + Z_2 \quad (14)$$

$$V_2 = Z_2 I_1 \quad (15)$$

Then according to (11):

$$Z_{21} = Z_2 = -j Z_0 \csc kl \quad (16)$$

Putting it into (13) then:

$$Z_1 = j Z_0 \csc kl - j Z_0 \cot kl = j Z_0 \tan kl / 2 \quad (17)$$

Because of the symmetry of the system $Z_3 = Z_1$.

Now that the two-port network is completed by combining two T-models and a third port is inserted into the system as an electrical port (Figure 6).

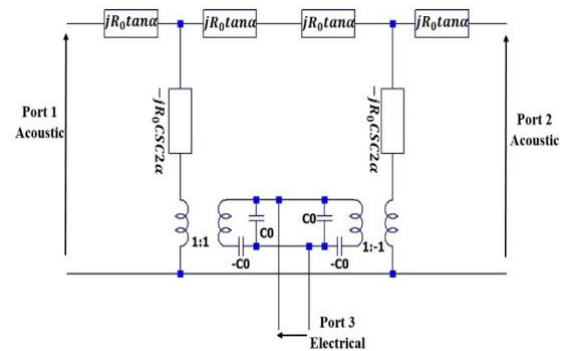


Figure 6. Mason equivalent circuit for each finger pair as a 3-port network. For In-Line approximation $-C_0$ is involved, for crossed-field model, it is short-circuited.

The model developed includes both “in-line” and “Cross-field” approximations in figure7 [12,14].

The only difference between the “in-line” and “crossed-field” model is that in the “crossed field” model –C0 is short circuited.

With $k = \frac{2\pi}{\lambda}$ and $l = \frac{\lambda}{2}$ we can define the following quantities, which were used on the model (Figure 6) (λ , ω , ω_0 shows wavelength, design frequency and the frequency of excitation signal respectively).

$$\alpha = \frac{kl}{2} \frac{\omega}{\omega_0} = \frac{\pi}{2} \frac{\omega}{\omega_0} , R_0 = Z_0, C_0 = \frac{C_s}{2}$$

C_s is the capacitance per length of the piezoelectric material.

For the ease of calculations, in-line model model was not preferred, we worked with the crossed field model. To come up with an equivalent circuit for the mathematical functions in the model, “Foster” method [16] was used. This approach involves creating a frequency versus impedance function by leveraging the positions and characteristics of zeros and poles in a network to formulate a circuit model. The objective is to design a circuit model that emulates the behavior of a SAW device. The equivalent circuit contains lumped (L, C) elements, which makes it perfect to use this model in an LTspice simulation.

1.2. Oscillator model (butterworth vandyke)

Considering the fact that the region of interest for a SAW device is around the resonance frequency, *Parker. Montress. el* [17] provided an equivalent circuit for the resonance behavior of the SAW device based on the mechanical behavior of the piezo electric material. This circuit perfectly describes the performance of a SAW device around resonance region. The mentioned equivalent circuit can be used only around resonance frequency and it could be used in a circuit to examine the oscillatory behavior of the circuit. Since SAW devices act as an LC tank, they are used in oscillator circuits as frequency determiner and such equivalent circuits make it easy to analyze the circuits using simulation software. Figure 7 shows the equivalent circuit for the resonance.

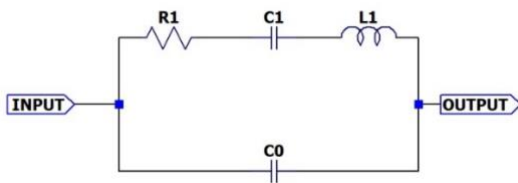


Figure 7. SAW device equivalent circuit

The values of the lumped elements can be easily calculated from experimental data to design an equivalent circuit.

The input admittance (Y_i) [18] is:

$$Y_i = \frac{j\omega^2 C_1 R_1 C_0 - (\omega C_0)(\omega^2 L_1 C_1 - 1) + \omega C_1}{R_1 \omega C_1 + j(\omega^2 L_1 C_1 - 1)} \tag{18}$$

Here, R_l, C_l and L_l are the model parameters representing mechanical motion and C_0 shows the static parameter. The whole structure models the behavior of a 1-port SAW device around the resonant region. The frequency variable is depicted by ω .

The equivalent circuit shows two resonances. At the series resonance f_s , the magnitude of Y_i is max. This gives us an equation where the imaginary part of the denominator is zero:

$$f_s = \frac{1}{2\pi \sqrt{L_1 C_1}} \tag{19}$$

Putting this into the Y_i will result:

$$Y_i(\omega_s) = \frac{1}{R_l} + j\omega_s C_0 \tag{20}$$

Given the input admittance at the series resonance frequency (ω_s) the resistance value of the equivalent circuit becomes:

$$R_1 = \frac{1}{Re(Y_i(\omega_s))} \tag{21}$$

Similarly, C_0 can be separated from the imaginary part of the input admittance at the resonance frequency.

$$C_0 = \frac{1}{2\pi f_s} imag(Y_i(\omega_s)) \tag{22}$$

At the parallel resonance (ω_p : the parallel resonance frequency), the input impedance of the circuit is maximum so the admittance is minimum. Setting the real part of the numerator in input admittance equation, to zero helps in finding the capacitance C_0 .

$$C_1 = C_0(\omega_p^2 L_1 C_1 - 1) = C_0 \left(\frac{\omega_p^2}{\omega_s^2} - 1 \right) \tag{23}$$

The value of the inductor L_1 from (11) is now easy.

Though the circuit gives a decent estimation of the behavior of a SAW device at resonance frequency it best suits the simulation of a SAW device in an oscillator circuit and is not designed to give any information about the number of fingers, length of the fingers and other design parameters.

1.3. Impulse response method

Instead of analyzing fingers using network models, the impulse response method works with the frequency response of the fingers due to their sizes [19-20]. Figure 8 shows that each gap between two fingers creates a half wave cycle and they add up together and create a whole wave that travels through the delay line to get to the receiver IDT.

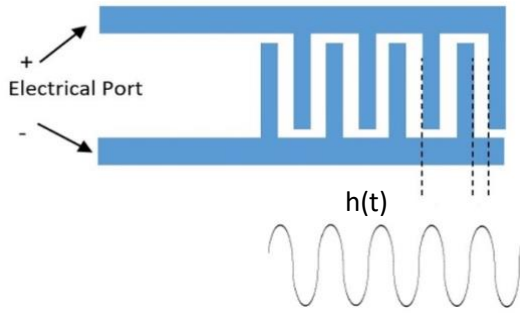


Figure 8. Geometry and impulse response

We know that the frequency response of this device is the Fourier transform of the impulse response :

$$H(\omega) = \int_{-\infty}^{+\infty} h(t)e^{-j\omega t} dt \quad (24)$$

In other words, the desired frequency response can be used to find the corresponding impulse response and design the fingers accordingly by using the inverse Fourier transform:

$$h(t) = \frac{1}{2\pi} \int_{-\infty}^{+\infty} H(\omega)e^{j\omega t} dt \quad (25)$$

taking $h(t)$ to be a sinusoidal function for simplifying the calculations, when an electrical impulse is given to the system, the amplitude of each half cycle is multiplied by $f_i^{\frac{3}{2}}$ where f_i is the instantaneous frequency [20]. So far, the impulse response is: $h(t) = f_i^{\frac{3}{2}} \sin\theta$. Here θ is the angle representing phase of the propagating wave at time t ,

$$\theta(t) = 2\pi \int_0^t f_i(\tau) d\tau \quad (26)$$

Where $t = \frac{x}{v}$ and v is the speed of wave in piezoelectric media. When there are N fingers involved then,

$$\theta = \omega_0 t \text{ and } f_i = f_0 \quad (27)$$

The amplitude $h(t)$ must be multiplied by a constant of the per finger capacitance C_s and the electromechanical coupling k :

$$h(t) = 4k\sqrt{C_s}f_0^{\frac{3}{2}} \sin\omega_0 t, \quad (28)$$

for $0 \leq t \leq \frac{N}{f_0}$

Performing the Fourier transform to get the frequency response, results in:

$$H(\omega) = 2k\sqrt{C_s}f_0 N \frac{\sin X}{X} e^{-j\frac{\omega N}{2f_0}}, \quad (29)$$

$$X = \frac{N\pi(\omega - \omega_0)}{\omega_0}$$

Once frequency response is determined, radiation conductance $G_a(\omega)$ and acoustic susceptance $B_a(\omega)$ are found respectively:

$$G_a(\omega) = 8k^2 C_s f_0 N^2 \frac{\sin^2 X}{X} = G_0 \frac{\sin^2 X}{X} \quad (30)$$

$$B_a(\omega) = \frac{G_0(\sin 2X - 2X)}{2X^2} \quad (31)$$

Having the acoustic conductance and susceptance can help finding the total admittance [21] of the IDT:

$$Y_i = G_a + j(2\pi f C_T + B_a) \quad (32)$$

C_T is the total capacitance which is the multiple of the number of finger pairs times the length of the fingers times the per length capacitance:

$$C_T = N_p \times C_s \times W_a \quad (33)$$

These relations can give the optimum length for the fingers to achieve the impedance matching between the IDT and input resistance [22]:

$$W_a = \frac{1}{R_{in}} \left(\frac{1}{2N_p C_s f_0} \right) \frac{(4k^2 N_p)}{(4k^2 N_p)^2 + \pi^2}, \quad (34)$$

where R_{in} shows the input resistance to be matched

II. BACKGROUND

LTspice is widely accessible and more importantly flexible in running AC analysis for lumped-element circuits with high precision and speed. Furthermore, the program allows the user to create blocks out of repeating parts, which perfectly suits circuits containing huge number of repeating parts. This in fact makes it a lot easier to draw the circuit and run analysis. At the end of each analysis, it is possible to save the data and later transfer them to any other program for further examination. All these and the user-friendly interface make LTspice a suitable option for the simulation.

A complete sender/receiver IDT pair simulation that clearly compares analytical and experimental results on a free access platform has not been available. This paper provides a full two IDT sender/receiver analysis where the number of finger pairs, length of fingers and

piezoelectric substrate are taken into consideration. We put the equivalent network of mathematical functions ($jZ_0 \tan \alpha$ and $-jZ_0 \csc \alpha$) into blocks and those blocks are easily called from the directory of the simulation file by the names TANEQ and CSCEQ. The equivalent circuits are shown in figure 9 and figure 10 [23]. These equivalent LC networks are calculated using “foster” method which was discussed in introduction section.

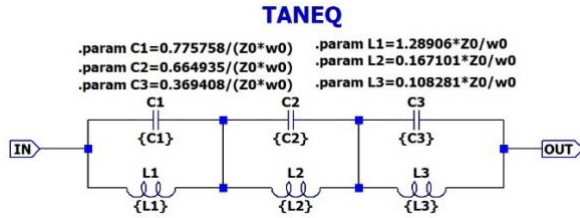


Figure 9. Equivalent circuit for $jZ_0 \tan \alpha$

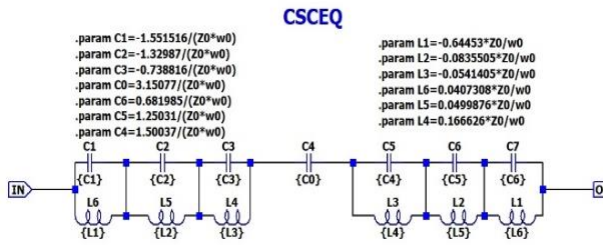


Figure 10. Equivalent circuit for $-jZ_0 \csc \alpha$

The blocks are useful to model the periodic fingers in the SAW devices. Mason model allows to model this periodicity by using each finger pair as a building block. The Mason equivalent circuit allows us to approximate the behavior of an IDT sender/Receiver pair within an acceptable margin. This model assumes that the finger overlap is constant; the width of every finger and the distance between neighboring fingers is constant and $\frac{\lambda}{4}$ as shown in figure 11. With this in mind, the center frequency of each device becomes $f_0 = \frac{v}{\lambda}$ where v is the wave speed in the piezoelectric material. The model also assumes that the metallization between fingers and spaces is 50%.

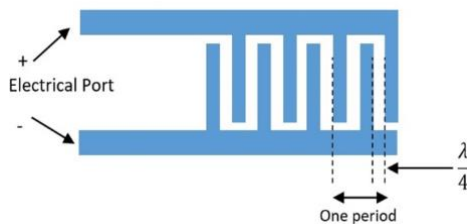


Figure 11. One period, one finger pair

2.1. Finger pairs

Every finger pair as shown in figure 11 is considered one period. The implementation of a finger pair in LTspice is demonstrated in figure 12. According to the Masons model, these fingers are acoustically in series connection and electrically parallel to each other. A 1:1 transformer shows the conversion from electrical energy to mechanical acoustical energy for each finger. Transformers are not defined in the LTspice as independent elements; however, inductors can be programmed to act as a transformer. To add to the overall Mason’s model, we added a resistor to the electrical input/output port of every finger of the both sender and receiver IDT to represent the ohmic losses due to the flow of current in the metal parts of the fingers. Since LTspice does not assume any resistance for the wires, this addition takes care of sudden spikes on the frequency response graph of the simulation result that does not appear in the actual network analyzer readings. The added resistances also help in stabilizing the phase, which resembles the experimental models more with the added resistance.

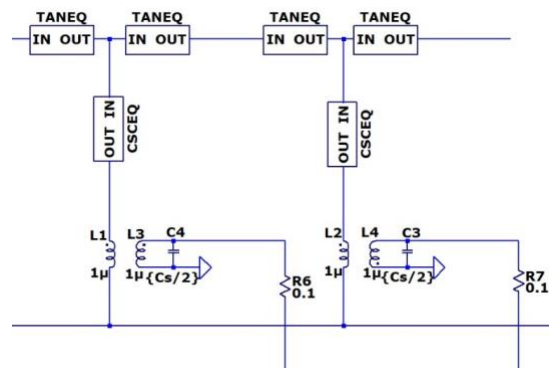


Figure 12. A finger pair in LTspice

III. THE COMPLETE MODEL, FABRICATION AND TEST

A complete equivalent system includes a sender and receiver IDT pair that are connected to each other. The mechanical output of the transmitter IDT is directly connected to the mechanical input of the receiver IDT block. The transmitter IDT model gives a voltage (V_t , Figure 13) representing the mechanical response of the IDT. Similarly, receiver IDT has input voltage source (V_r , Figure 13) depending on the mechanical vibrations coming from transmitter IDT (these vibrations are modeled using V_t voltage). The V_r - V_t relationship is a function of the frequency of the system, capacitance per length and coupling factor of the piezoelectric material. *Krairojananan and Redwoodthan et* [24] offers such

function for the receiver (detector) IDT shown on figure 13 that shows a satisfactory compatibility with the experimental data. This function is easily implemented in LTspice using the dependent voltage source.

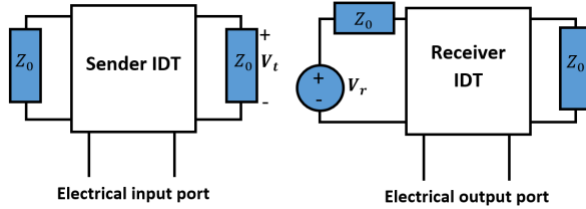


Figure 13. Two port SAW Device IDT

$$V_r = V_t \left\{ \frac{1}{2} \left(\frac{9k^2}{4\pi} \right) (\omega_0 C_s Z_0) \right\}^{0.5} \quad (35)$$

The electrical ports of all receiver IDT fingers are connected at the end and grounded with a 50-ohm resistance that acts like the ports of a network analyzer to provide a node for LTspice to plot the output voltage from that node. Receiver IDTs have the same configuration as the sender IDTs that are terminated by intrinsic impedances and LTspice allows copying the design. Based on the number of finger pairs in the design the corresponding circuit could be created and LTspice performs the AC analysis.

3.1. The simulation and fabrication parameters

The model is tested through the LT spice simulations and the results are verified by the experimental data. A system containing transmitter and receiver IDTs with 13 pairs of fingers on each was used. The IDTs were grown on a LiNbO3 y-z cut substrate material because of its relatively better electromechanical coupling capability. The design wavelength is $\lambda=100 \mu\text{m}$ that results in the operation frequency around 39.9 MHz. The length of each finger is about 27λ ($2748.22\mu\text{m}$) to ensure that the generated wave is flat enough. The distance between two IDTs was chosen as 1.2 mm, to have a reasonable attenuation (Table-1).

Table 1. Simulation and fabrication parameters

Parameter	Value
Saw Speed(m/s)	3990 m/s
Wavelength (μm)	100
Frequency(MHz)	39.9
Aperture size (mm)	2.75
Metallization Factor	50%
Delay Line Length (mm)	1.2
Number of Fingers	13
Substrate Material	lithium niobate y-z cut

Cs (capacitance per length) for Lithium Niobate is obtained using tensile dielectric constants described by *Engen et al* [25]. In this method, a parameter containing both capacitance per length and dielectric constants of the material is related to the metallization factor of the design. For the metallization factor of 0.5 in our design, the parameter is 20. Putting it into the relation defined in [25]:

$$20 = \frac{C_s}{0.5(1+\epsilon_r \frac{\epsilon_{33}}{\epsilon_0})} \quad (36)$$

$$\text{With } \epsilon_r = \sqrt{\frac{\epsilon_{11} - \epsilon_{13}^2}{\epsilon_{33} - \epsilon_{33}^2}} \quad (37)$$

Here, ϵ_r is relative permittivity and ϵ_{ij} are relative permittivity in different directions in the material. The values of dielectric constants are provided by *R. S. Weis and T. K. Gaylord et al* [26]. One must be careful in selecting the correct value of the dielectric constant with respect to the nature of the wave propagated in the medium as lithium niobate has shear and tensile dielectric constants. Since our device is propagating Rayleigh waves, then tensile dielectric constants are used which results in the capacitance per length of 512 pf/m. The simulation was performed between 20-60MHz interval with 400 points per decade.

3.2. Fabrication

Several piezo electric substrates are used to fabricate SAW devices such as ST-Quartz, Lithium Niobate and Lithium tantalite. Depending on the application of the sensor, whether it is designed to produce Rayleigh wave or shear-horizontal waves, different cuts of the materials are used. Among those Lithium niobate offers a good electromechanical coupling and fair price. Higher electromechanical coupling means that the piezoelectric material is more responsive to the electrical signal and this makes working with lithium niobate easier.

The parameters have selected to meet the same device properties as in the LTspice model for fair comparison. Since the SAW velocity on LiNbO3 substrate is about 3990 m/s, the finger-finger distance of an IDT electrode is selected as $100 \mu\text{m}$ to have a resonance frequency around 39.90 MHz. The design wavelength is $100 \mu\text{m}$, which defines the aperture length and the width of each IDT electrode fingers. The fingers' width is $25 \mu\text{m}$ that corresponds to 50% metallization ratio (Fig. 11). The aperture length is used as 50-wavelengths to generate plane waves. The distance between the transmitter and receiver IDT electrodes is 1.2 mm, providing a mechanical-wave attenuation around 12 dB (Fig. 16a).

The fabrication of the SAW device uses a six-step process (Figure 14). The LiNbO₃ wafer is meticulously washed with acetone and later with distilled water and methanol to clean the surface then the wafer is placed into ultrasonic washing bath device for 10 minutes to be sure the surface cleanness. In the second step chrome is deposited on the surface using DC sputtering device for 30 minutes at 500 mA current to have 200 nm chromium film on the substrate. After depositing chrome on the surface of the lithium niobate wafer, the photoresist AZ5214E is placed on the wafer and then the wafer is spun for 45 seconds with the speed of 4000 rpm and the acceleration of 1500 rpm/sec. The photoresist thickness is 1 μm . The wafer is baked for 50 seconds at 105 $^{\circ}\text{C}$ before UV exposure. The wafer is put the developer solution after 7 seconds UV exposure; the exposed parts separate and leave the chrome on the surface. Then, the wafer is put inside the chromium etch solution (Cr01), to etch away the chromium that exposed to UV light. After this step, the electrodes are ready, however on top of them there are still some photoresist materials that should also be washed away with acetone. The fabricated SAW device can be seen in Figure 15.

The fabricated device is then connected to the network analyzer to examine its frequency response. Before connecting the device to a network analyzer, the network analyzer is calibrated around the center frequency.

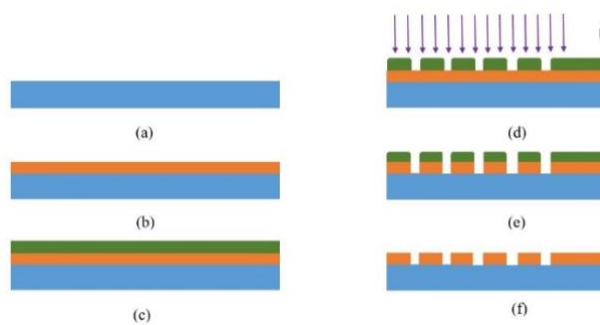


Figure 14. Fabrication steps: a) Clean the substrate. b) Chromium sputtering, c) photoresist layer, d) Lithography, e) Developer, f) Acetone rinse

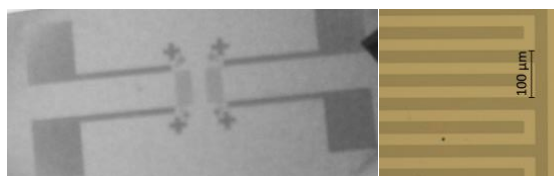


Figure 15. a. Fabricated 2-port SAW device, b. magnified view of the electrode fingers.

3.3. Stability Analysis

The stability of a specific parameter in a Surface Acoustic Wave (SAW) device becomes critical if the device is not explicitly designed to sense some physical or chemical quantity. Usually, it is essential to maintain stability in the resonance frequency under diverse environmental conditions, including variations in temperature, pressure, chemical exposure, and mechanical stress.

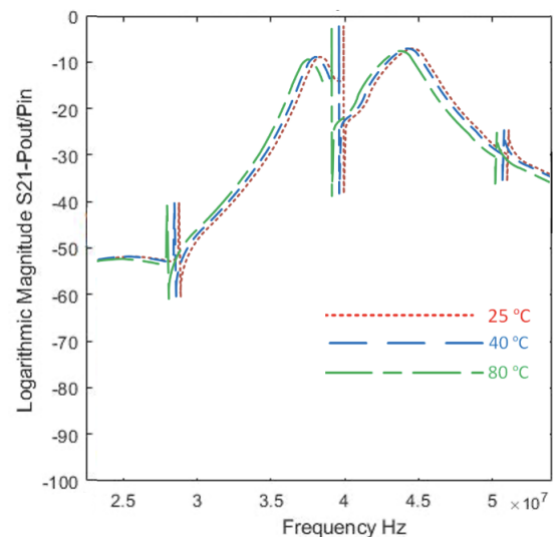


Figure 16. The temperature stability analysis of the fabricated device.

Temperature stability is typically a critical factor, as piezoelectric materials often exhibit variations in their electrical response with fluctuating temperature conditions. In this study, the temperature stability for the fabricated SAW device was analyzed by measuring its frequency response (s_{21} parameter) under three different temperature conditions. The SAW device is placed within a oven (Despatch LCC1-16-3 HEPA) while connected to a vector network analyzer (Copper Mountain, Indianapolis, USA), capturing the frequency response in the vicinity of the resonance region. The frequency response is recorded following a 30-minute period to ensure a consistent temperature. Three frequency responses have provided for 25 $^{\circ}\text{C}$, 40 $^{\circ}\text{C}$ and 80 $^{\circ}\text{C}$ temperatures values.

V. RESULTS AND DISCUSSION

The S_{21} parameter was measured under various temperature conditions using a vector network analyzer (Copper Mountain, Indianapolis, USA). An analysis of temperature stability revealed that the resonance frequency slightly decreased with rising temperatures (Figure 16). Additionally, there was a negligible increase in the attenuation value. Specifically, the

resonance frequencies were observed at 39.915 MHz, 39.886 MHz, and 39.835 MHz at temperatures of 25°C, 40°C, and 80°C, respectively. The observed frequency shift between 25°C and 80°C is 0.2%, which corresponds to temperature coefficient of frequency value (TCF) of -36.4 ppm/°C (38).

$$TCF \left(\frac{ppm}{^\circ C} \right) = \frac{f_{ri} - f_r}{\Delta T \times f_r} \times 10^6 \quad (38)$$

,where f_r and f_{ri} are the resonance frequencies measured at 25 °C and 25 °C+ΔT, respectively. The temperature difference is given by ΔT. The value that is experimentally found aligns closely with findings in the literature [27,28].

The frequency response result from the LTSpice model is represented in Figure 17, here the resonance peak can be clearly seen at 38.405 MHz in the magnitude response. The phase change around the resonance frequency also shows the resonance at the same frequency.

Another result involves a comparison of the frequency responses between the fabricated device and the LTSpice model, both sharing identical design parameters. The frequency responses of the manufactured SAW device and the LTSpice model are illustrated in Figure 18a, revealing resonance peaks at 39.915 MHz and 38.405 MHz, respectively. Furthermore, the phase responses are agreed and the phase change around the resonance frequency shows the resonance at the same frequency (Figure 18b).

The experiments and the Ltpspice model have the same magnitude peaks at the resonance frequency and the phase change occurs in the resonance frequency for both results.

LTspice provides easy to use environment to test the electronic circuits before the production of prototypes. The results shows that the Ltpspice model for the SAW device has the same behavior and it allows complete simulation of the circuits with SAW devices.

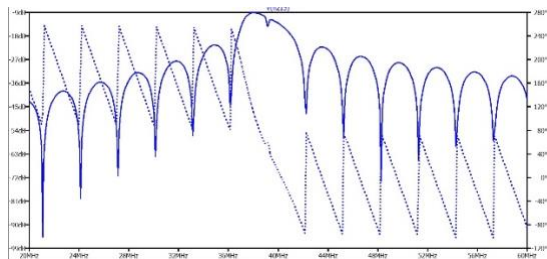


Figure 17. Output readings of the sender/Receiver IDT pair from simulation.

VI. CONCLUSION

In this study, a complete model simulation of a 13-finger pair transmitter/Receiver IDT was run on LTspice and compared with the fabricated device. The results show a conspicuous agreement between the simulated LTspice model and experimental data. As a result, the model can be used to accurately predict the response of a design before fabrication to achieve the optimum desired performance. The capability to simulate any SAW device in a circuit (such as an oscillator) using the LTspice model is also demonstrated in the study.

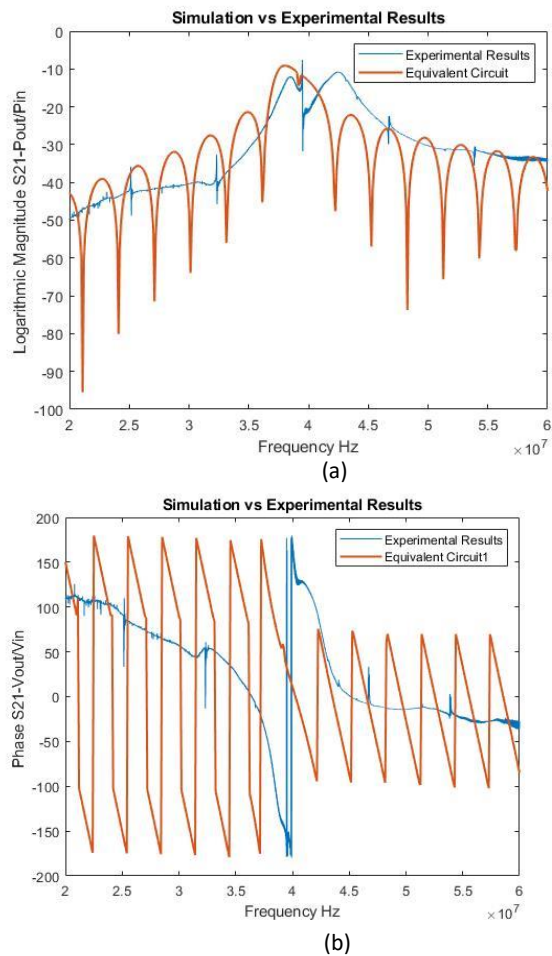


Figure 18. a) Log Mag comparison of experimental and simulation results b) Phase comparison of experimental and simulation results

REFERENCES

- [1] Rayleigh, L. (1885). On Waves Propagated along the Plane Surface of an Elastic Solid. Proceedings of the London Mathematical Society, s1-17(1), 4–11. <https://doi.org/10.1112/plms/s1-17.1.4>
- [2] Stoneley, R. (1924). Elastic waves at the surface of separation of two solids. Proceedings of the

- Royal Society of London, 106(738), 416–428. <https://doi.org/10.1098/rspa.1924.0079>
- [3] Ingebrigsten K.A.,(1967). Elastic surface waves in piezoelectrics and their coupling to carriers in an adjoining semiconductor. *Elab Rept TE-94* Norwegian Institute of technology, Trondheim, Norway., 1(1).
- [4] Strauss, W. A. (1965). Magnetoelastic waves in yttrium iron garnet. *Journal of Applied Physics*, 36(1), 118–123. <https://doi.org/10.1063/1.1713856>
- [5] Fall, D., Duquennoy, M., Ouafthouh, M., Piwakowski, B., & Jenot, F. (2018). Effective and rapid technique for temporal response modeling of surface acoustic wave interdigital transducers. *Ultrasonics*, 82, 371–378. <https://doi.org/10.1016/j.ultras.2017.09.018>
- [6] Kamal, A., Ali, M. a. A., Faris, M., Monzer, O., & Mostafa, H. (2020). Design and analysis of Multi-Port SAW MEMS resonators. 2020 9th International Conference on Modern Circuits and Systems Technologies (MOCASST),1-4. <https://doi.org/10.1109/mocast49295.2020.9200258>
- [7] Pennuri, D., et al. (2003). A Circuit Simulation Component Model For RF Surface Acoustic Wave Devices. In *S3 2003 Symposium (Motorola)*.
- [8] Hagmann, M. J. (2019). Analysis and equivalent circuit for accurate wideband calculations of the impedance for a piezoelectric transducer having loss. *AIP Advances*, 9(8), 085313.
- [9] Yazdani, M. A., & Sisman, A. (2020). A novel numerical model to simulate acoustofluidic particle manipulation. *Phys. Scr.*, 95, 095002.
- [10] Elsherbini, et al. (2016). Finite Element Method Simulation for SAW Resonator-Based Sensors. *International Electrical Engineering Journal (IEEJ)*, 7(2), 2167-2172.
- [11] Mason, W. P. (1942). *Electromechanical Transducers and Wave Filters*. New York.
- [12] Smith, W. R., Gerard, H. M., Collins, J. H., Reeder, T. M., & Shaw, H. J. (1969). Analysis of Interdigital Surface Wave Transducers by Use of an Equivalent Circuit Model. *IEEE Transactions on Microwave Theory and Techniques*, MTT-17(11).
- [13] Berlincourt, D. A., Curran, D. R., & Jaffe, H. (1964). In W. P. Mason (Ed.), *Physical Acoustics* (Vol. 1A, pp. 233-242). New York: Academic Press.
- [14] Hoang, T. (2011). SAW Parameters Analysis and equivalent circuit of SAW device. In *InTech eBooks*. <https://doi.org/10.5772/19910>
- [15] Mishra, D., Hussain, D. M. A., Dhankar, M., Singh, A., & Dabas, S. (2016). *Interdigital Transducer Modeling through Mason Equivalent Circuit Model Design and Simulation*.
- [16] Ryder, J. D. (1964). *Networks, Lines, and Fields*. Asia Publishing House, pp. 80-88.
- [17] Parker, T. E., Montress, G. K. (1988, May). *Precision Surface Acoustic Wave (SAW) Oscillator*.
- [18] Huang, H., Paramo, D. (2011, December). *Broadband Electrical Impedance Matching for Piezoelectric Ultrasound Transducer*.
- [19] Fall, D., Duquennoy, M., Ouafthouh, M., Piwakowski, B., & Jenot, F. (2015). Modelling based on Spatial Impulse Response Model for Optimization of Inter Digital Transducers (SAW Sensors) for Non Destructive Testing. *Physics Procedia*, 70, 927–931. <https://doi.org/10.1016/j.phpro.2015.08.192>
- [20] Hartmann, C. S., Bell, D. T., & Rosenfeld, R. C. (1973). Impulse Model Design of Acoustic Surface-Wave Filters. *IEEE Transactions on Microwave Theory and Techniques*, 21(4), 162-175. doi:10.1109/TMTT.1973.112
- [21] Lakin, K. M., Joseph, T., & Penunuri, D. (1974, November). Planar Surface Acoustic Wave Resonator. *Ultrasonic Symposium Proceedings, IEEE*, 1, 263-267.
- [22] Wilson, W. C., & Atkinson, G. M. (2006, October). Mixed modeling of a SAW delay line using VHDL.
- [23] Fu, Q., Fischer, W., & Stab, H. (2003, May). *Simulate Surface Acoustic Wave Devices Using VHDL-ALM*.
- [24] Krairojananan, T., & Redwood, M. (1971, February). Equivalent electrical circuits of interdigital transducers for piezoelectric generation and detection of Rayleigh waves. *Proceedings of the Institution of Electrical Engineers*, 118(2), 305-310.
- [25] Engen, H. (1969, April). Excitation of Elastic Surface Wave by Spatial Harmonics of Interdigital Transducers. Norwegian Institute of Technology, Trondheim, Norway.
- [26] Weis, R. S., & Gaylord, T. K. (1985, March). *Lithium Niobate: Summary of Physical Properties and Crystal Structure*. School of Electrical Engineering, Georgia Institute of Technology, Atlanta, GA.
- [27] Hage-Ali, C. S., et al. (2020). FEM Modeling of the Temperature Influence on the Performance of SAW Sensors Operating at GigaHertz Frequency Range and at High Temperature Up to 500°C. *Sensors*, 20(15), 4166. doi:10.3390/s20154166.

-
- [28] Hickemell, F. S., et al. (1995). The surface acoustic wave propagation characteristics of 64° Y-X LiNbO₃ and 36° Y-X LiTaO₃ substrates with thin-film SiO₂. In 1995 IEEE Ultrasonics Symposium. Proceedings. An International Symposium (Vol. 1, pp. 345-348).